Coexistence of Superconductivity and Short-Range Magnetic Order*

L. J. Williams,† W. R. Decker,‡ and D. K. Finnemore

Institute for Atomic Research and Department of Physics, Iowa State University, Ames, Iowa 50010

(Received 30 March 1970)

Thermal conductivity measurements on the La-Lu-Tb alloy system show that short-range magnetic order in the magnetic-impurity spin system does not change the superconducting properties in a substantial way. There appears to be no anomaly in the thermal conductivity at the temperature where short-range order occurs. The critical-field curves are depressed far below the prediction of the multiple-pair-breaking theories, and this seems to indicate the presence of a strong exchange-field enhancement.

INTRODUCTION

Bennemann and Mueller[1] have predicted that the ordering of magnetic impurities in a superconductor might give rise to an anomaly in the superconducting electronic thermal conductivity (λ_{es}) at the magnetic ordering temperature T_0. Within the framework of their theory there are two main contributing factors. First, the magnetic ordering will tend to decrease the spin-flip scattering and this will cause a decrease in λ_{es} at the ordering temperature. Second, the magnetic ordering will introduce a molecular field which will Zeeman split the Fermi surface and this will cause a rise in λ_{es} at the ordering temperature. Spin-orbit scattering can moderate the molecular-field effect, but it will not change the spin-flip scattering. Hence, a sample with a large spin-orbit scattering time τ_{so} might show an anomalous rise in λ_{es} at T_0, and a sample with a small τ_{so} might show an anomalous drop in λ_{es} at T_0. The purpose of the work reported here was to look for such an anomaly in the La-Lu-Tb alloy system.

Earlier measurements on Th-Gd[2] have verified that the Abrikosov-Gor'kov and Ambegaokar-Griffin theory[3] is well satisfied for the circumstance when the magnetic impurities are known to be paramagnetic. For the work described here, an alloy system was chosen which shows superconductivity with the magnetic impurities in both the paramagnetic and the ordered state.[4] The La-Lu was chosen for the host material because there were both neutron-diffraction and susceptibility data[5] available for these alloys. The addition of a small amount of Lu guarantees that the samples are always in the type-II region, and it also helps stabilize the d-hcp crystal structure. An early attempt to use $La_{80}Lu_{20}$ as the host material was unsuccessful because the phonon conductivity is comparable to the electronic conductivity near 4 °K. It was found, however, that decreasing the Lu content enhances the electronic conductivity, and it also diminishes the phonon conductivity substantially. $La_{98}Lu_2$ was chosen for the host.

A superconductivity and magnetic-order phase diagram for this system is shown in Fig. 1. The $La_{98}Lu_{1.15}Tb_{0.85}$ sample goes superconducting at 2.718 °K and magnetic order occurs at about 1.3 °K. The $La_{98}Lu_1Tb_1$ sample goes superconducting at 2.108 °K and T_0 is about 1.5 °K. Even though the magnetic-ordering phase transition is rather broad, there is still a substantial superconducting region in which the magnetic impurities are approximately paramagnetic (2.8–1.3 °K) and another large region in which the magnetic impurities show a short-range order (1.3–0.3 °K).

EXPERIMENTAL

Sample Preparation

The rare-earth metals used to prepare these samples were provided by Spedding's group of Ames Laboratory. A spark-source mass-spectrographic analysis shows that H, C, N, O, and F were the major impurity constituents at 18, 40, 193, 219, and 70 ppm by weight, respectively.

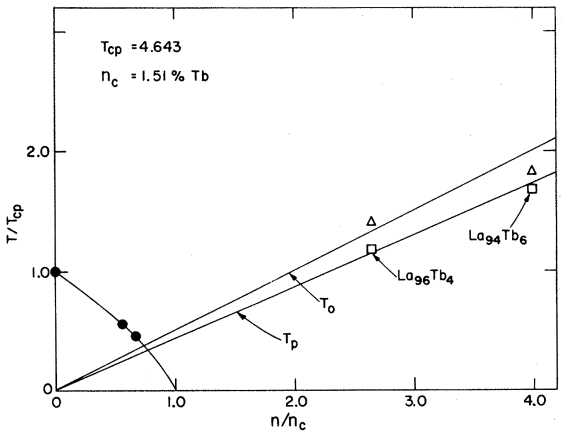

FIG. 1. Superconducting and magnetic-order phase diagram for the La-Lu-Tb system.

Fe at 10 ppm and Pr at 30 ppm were the only important magnetic-impurity components. Other impurities were less abundant.

Master alloys of $La_{80}Lu_{20}$ and $La_{80}Tb_{20}$ were prepared by arc melting in a He atmosphere on a water-cooled copper mold. Pieces of these master alloys were then cut with a jewelers saw, electropolished in a perchloric-acid–methanol solution, and arc melted in a finger-shaped mold. Each sample was turned over and remelted 10 times to ensure homogeneity. After melting, this sample was spark cut into a piece about 3 in. long with a cross section of 0.14 in. by 0.14 in. The carbonized surface was then removed with a carbide file and the sample was electropolished until shiny. It was swaged, with one pass, into a cylindrical rod 0.137 in. in diam and electropolished again. To anneal the sample it was sealed under He in an outgassed Ta tube and this tube was in turn sealed inside a glass tube. The entire assembly was placed in an oven for the annealing. Sample 1 ($La_{98}Lu_2$) was annealed for 10 h at 250 °C and then for 151 h at 220 °C. Sample 2 ($La_{98}Lu_{1.15}Tb_{0.85}$) was annealed for 60 h at 250 °C. Sample 3 ($La_{98}Lu_1Tb_1$) was annealed for 190 h at 250 °C.

Unfortunately, sample 3 was partially damaged when it was being sealed in the Ta tube, and so this sample was somewhat shorter than the others. One end was melted and fused into the Ta in the process of welding the tube. Most of the sample appeared to be unaffected, however, and the damaged portion was cut away. In the spectrographic analysis after sample preparation, Ta was not detected in this sample. A neutron-diffraction study of the crystal structure of these samples showed that the "as-cast" material contained about 6% fcc and 94% d-hcp. After the annealing, the fcc component dropped to less than 1.6%. A final step in the sample analysis was to observe the grain structure visually with 250× magnification cross section parallel to and including the axis of the cylindrical specimen. There was a noticeable decrease in grain size toward the outer edge of the sample, presumably due to preferential cold working in the swaging process. Samples 1 and 3 had a grain size of about 2×10^{-5} cm and sample 2 had a grain size of about 3×10^{-6} cm. Sample 2 also showed much heavier faulting.

Equipment

Thermal conductivity data were taken with a four-probe technique in the He^3 cryostat shown in Fig. 2. This is basically the same apparatus used for the critical-field experiment reported earlier.[6] A germanium resistor GR 928 was calibrated against the vapor pressure of He^4 in the 4.2 to 1.5 °K range and it was calibrated against the susceptibility of cerium magnesium nitrate in the 1.5 to 0.3 °K range. For the thermal conductivity measurements we used matched Speer carbon resistors (SRC and SRH) and calibrated them on each run against GR 928. All of these resistors showed some magnetoresistance; therefore, they were suspended below the sample on the end of No. -16 Cu wire in a region where the magnetic field was $\frac{1}{6}$ the field of the sample (see Fig. 2). The largest field used was 11 500 Oe at the sample, and this would give 1700 Oe at the resistor. At 0.3 °K, 1700 Oe would change the resistance of a carbon resistor by about 0.3% and this corresponds to a temperature error of 0.0007 °K. These errors tend to cancel in the temperature difference across the sample, so magnetoresistance does not introduce important errors at these fields. For samples 2 and 3, the fields were a factor of 5 smaller; therefore, it is a completely negligible effect for these cases.

Electrical-resistance measurements on GR928 were made potentiometrically with a four-probe dc technique. The resistance of the carbon resis-

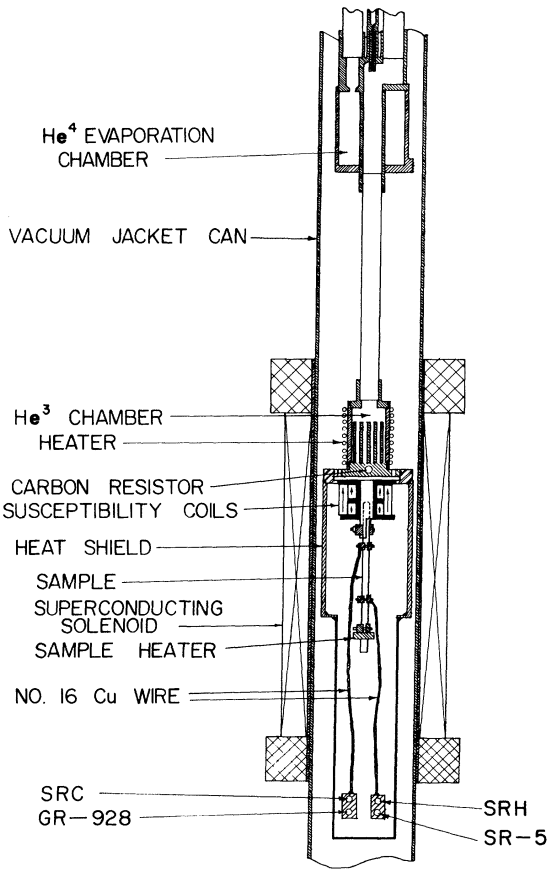

FIG. 2. Cryostat drawing.

tors was measured with a 32-Hz Wheatstone bridge. The bridge could be arranged to measure SRC, SRH, or the difference SRC minus SRH by placing the resistors in appropriate arms of a Wheatstone bridge. To measure SRC minus SRH the two resistors are placed in opposite arms of the bridge. Many errors tend to cancel in the difference, so a direct measurement of SRC minus SRH gives a precision in the thermalconductivity data four times better than a subtraction of the measured values of SRC and SRH.

A complicating feature of these measurements is that the thermal conductivity changes by more than two orders of magnitude in the 4.2 to 0.3 °K range. To obtain sufficiently accurate data at high temperatures, it was necessary to choose an area-to-length ratio for the sample, which gives a very large thermal resistance at low temperatures. Hence, it was especially important to keep heat leaks small at low temperature. For example, a heat leak of 1 erg/sec would cause a temperature gradient of several hundredths of a Kelvin at the lowest temperature for sample 1. Before each run we made an approximate measurement of the heat leak by noting the temperature difference between the hot and cold ends in both the superconducting and normal states to be sure that the heat leak was low. In the temperature ranges where heat leaks were a measurable effect, data were taken with both zero heater power and an applied heater power so that this correction could be made.

RESULTS AND DISCUSSION

Normal-State Data

Thermal conductivity data for each of these samples are shown in Figs. 3(a)–3(c). For the normal state (open triangles), the electrons are the primary carriers of heat and the impurities are the dominant scattering mechanism, so that the leading term has a linear temperature dependence. There is also a small phonon conductivity indicated by the upward curvature at higher temperatures. In the analysis of these data, we have assumed that the phonons are predominantly scattered by dislocations and by electrons. Both of these mechanisms give a T^2 term in the phonon conductivity; therefore the total conductivity data have been fit to an equation of the form

$$\lambda_n = AT + BT^2 . \qquad (1)$$

The leading term here is interpreted as the electronic contribution (λ_{en}) and the second term is the phonon conductivity (λ_{gn}). More complicated analyses including boundary scattering, etc., have been tried, but these terms are small and cannot reliably be separated for the normal-state data. The

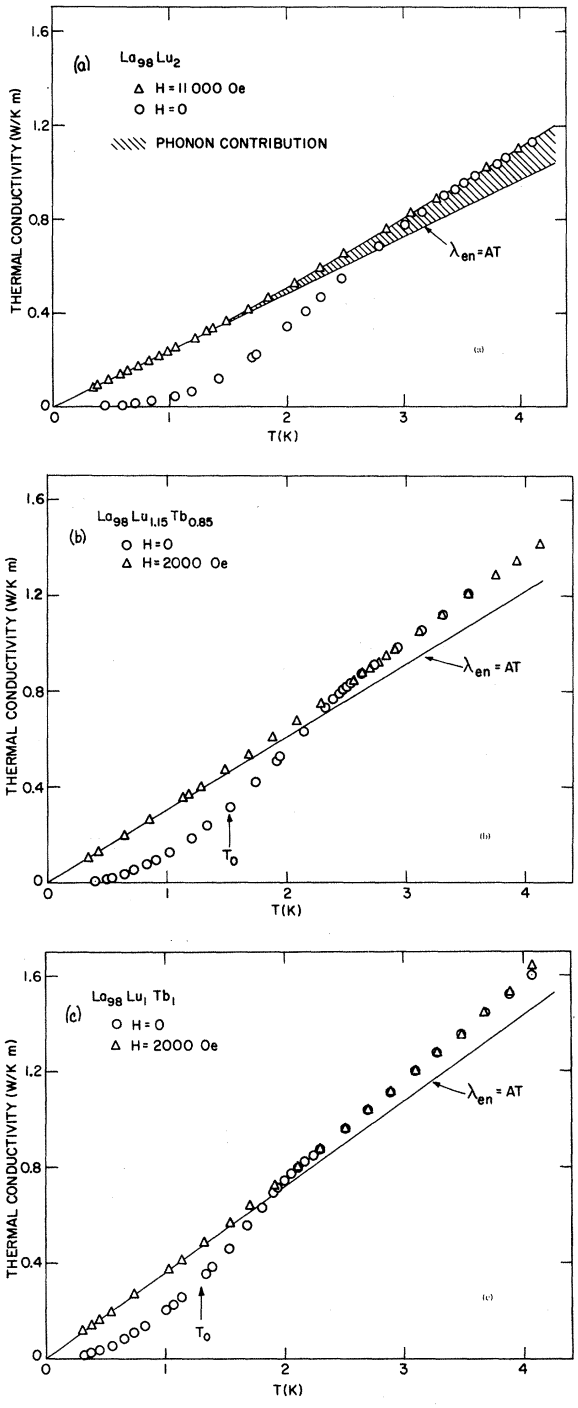

FIG. 3. Superconducting and normal-state thermal conductivity for three samples. Shaded area shows the normal-state phonon conductivity for sample 1.

data fit Eq. (1) with an rms deviation of $\frac{3}{4}\%$ for the values of A and B given in Table I. The Lorentz number L determined from λ_{en} and the electrical resistivity by

TABLE I. Properties of lanthanum-lutetium-terbium alloys.

Property	Sample 1	Sample 2	Sample 3
Composition	$La_{98}Lu_2$	$La_{98}Lu_{1.15}Tb_{0.85}$	$La_{98}Lu_{1.00}Tb_{1.00}$
$\rho_{300}(\mu\Omega\,\mathrm{cm})$	67.23	65.72	59.58
$\rho_{4.2}(\mu\Omega\,\mathrm{cm})$	9.979	7.343	6.390
$A(\mathrm{W/K^2\ m})$	0.2304	0.303 4	0.359 5
$B(\mathrm{W/K^3\ m})$	0.01148	0.010 52	0.008 65
$L(10^8\mathrm{W\Omega/K^2})$	2.30	2.23	2.30
T_c(K)	4.643	2.582	2.108
T_0	•••	~1.3	~1.5
H_{c30} (Oe)	11 500	1380	820
κ	5.75	4.41	3.93
$\Gamma/\Delta_p(0)$	0	0.279	0.334

$$L = \lambda_{en}\rho_0/T = A\rho_0$$

is about 2.3×10^{-8} $\mathrm{W\Omega K^{-2}}$(see Table I) compared to a free-electron value of $2.45\times10^{-8}\mathrm{W\Omega K^{-2}}$. This close agreement lends further support to the validity of the above separation. A pictorial view of the relative magnitudes of the phonon and electronic conductivities is shown by the shading in Fig. 3(a). For samples 2 and 3, the phonons contribute a smaller fraction of the total conductivity.

In the early stages of this work it was hoped that the normal-state conductivities of the three samples would be nearly the same because the total number of impurity atoms was fixed at 2%. This is not the case. The electronic conductivity increases and the phonon conductivity decreases as Lu atoms are replaced by Tb atoms. Presumably Lu impurities have a scattering cross section for conduction electrons in a La host which is about twice as large as that of Tb impurities. This increase in electron mean-free path causes an enhancement of the electron-phonon interaction which in turn decreases the phonon-mean-free path.[7] Another factor contributing to the variation in normal-state behavior was the very small grain size for sample 2. Despite these variations, the Lorentz number is close to this free-electron value for all samples, and there is a close similarity in the normal-state behavior.

Superconducting-State Data

Superconducting transition temperatures for these samples have been determined from 32-Hz susceptibility data. As determined by this ac technique, the phase transitions are about 0.035 °K wide for samples 1 and 3 and about 0.070 °K wide for sample 2. This greater width for sample 2 is probably related to the smaller grain size. These results are shown as the open circles in Fig. 1 and are listed in Table I.

A cursory look at the raw superconducting thermal conductivity data in Figs. 3(b) and 3(c) shows no bumps or wiggles in the region of T_0 of the sort envisioned by Bennemann and Mueller.[1] To show this more clearly, the data are plotted in the form of the ratio λ_s/λ_n versus $t = T/T_c$ in Fig. 4. A first impression is that there is no anomalous enhancement or depression of the conductivity at T_0. However, a full understanding of the data requires an analysis of the phonon contribution to decide whether there might be a coincidence in which a bump in the phonon conductivity would just cancel the expected bump in the electronic conductivity. Hence, it is important to make a fairly careful study of the phonon conductivity.

A complete analysis of the phonon conductivity involves many adjustable parameters, and it is difficult to make a unique interpretation of the results. Hence, our approach has been to determine upper- and lower-bound curves by making some fairly reasonable assumptions. The general approach is to analyze the phonon in the host materi-

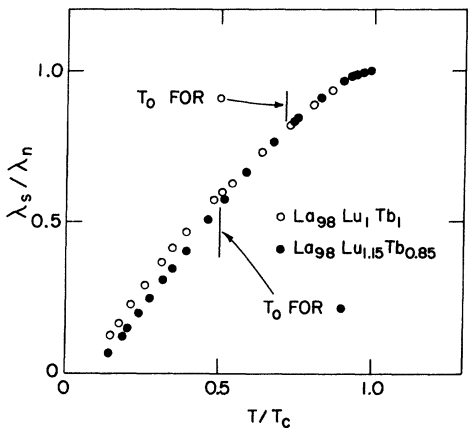

FIG. 4. Ratio of superconducting to normal thermal conductivities.

al where the electronic conductivity is fairly well understood[8] and then use the host-phonon contributions as a guide to determine Tb-alloy phonons. The following notation will be adopted in discussing these calculations: A subscript e or g denotes whether the carriers are electrons or phonons. The subscript s or n denotes whether the sample is superconducting or normal. These subscripts are separated by a slash from another subscript which indicates whether the scattering is due to electrons e, phonons g, point defects p, dislocations d, grain boundaries b, or sample boundaries l. For example, the normal-state phonon conductivity limited by electron scattering would be denoted by $\lambda_{gn/e}$. The work of Klemens[9] and Slack[10] has been the guide for the temperature dependence of each contribution.

For the host sample, the following prescription has been used to determine the various contributions to the phonon conductivity. λ_{en} is determined from the measured λ_n value by a least-squares fit to Eq. (1). λ_{gn} is determined from $\lambda_{gn} = \lambda_n - AT$. λ_{es} is determined from λ_{en} via the Bardeen, Rickayzen, and Tewordt[8] (BRT) theory with an effective energy gap of $3.70\ kT_c$. λ_{gs} is determined from $\lambda_{gs} = \lambda_s - \lambda_{es}$. These λ_{gs} data are then fit to an equation of the form

$$\lambda_{gs}^{-1} = \lambda_{gs/e}^{-1} + \lambda_{gs/p}^{-1} + \lambda_{gs/d}^{-1} + \lambda_{gs/b}^{-1}$$

or

$$\lambda_{gs}^{-1} = (R_g B_e T^2)^{-1} + (B_p T)^{-1} + (B_d T^2)^{-1} + (B_b T^3)^{-1}.$$

R_g is the BRT ratio for $\lambda_{gs/e}$ to $\lambda_{gn/e}$. A computer is then used to minimize the rms deviation and the best fit is found for $B_d = 1.107$, $B_b = 0.714$, $B_p = 0.023$, and $B_e = 0.161$. The relative magnitude of these constants implies that electron scattering of phonons is not very important in the normal state (approximately a 16% effect at $1.0\,^\circ K$), but it can dominate in the superconducting state because of the R_g factor. A more detailed discussion of this analysis is given elsewhere.[11]

For the Tb alloys, we have assumed that the point-defect boundary dislocation scattering terms are the same as in the host. The amount of electron scattering of phonons ($\lambda_{gn/e}$) is then adjusted to give the correct measured phonon conductivity in the normal state. At this point one would like to calculate $\lambda_{gs/e}$ but unfortunately there is no theory which gives R_g for the paramagnetic impurity case. Failure to have information on this factor is a major uncertainty in this analysis. We know, however, that this R_g factor will lie somewhere between the BRT value and 1 ($R_g = 1$) so at least we can bracket the region of λ_{gs}. If λ_{gs} is computed using $R_g = 1$ for all temperatures, then an upper-bound curve can be computed for $\lambda_{es}/\lambda_{en}$ [open circles in Fig. 5(a)]. This curve agrees rather well with the Ambegaokar-Griffin (AG) theory[3] shown by the solid line. If λ_{gs} is computed using the R_g given by BRT, then a lower-bound curve can be computed for $\lambda_{es}/\lambda_{en}$ [open triangles in Fig. 5(a)]. This curve lies well below the AG[3] curve even in the paramagnetic region where there has been experimental confirmation of the theory.[2] In addition, the position of the shoulder of the $\lambda_{es}/\lambda_{en}$ curve does not seem to correlate with the ordering temperature T_0. Hence, we think the

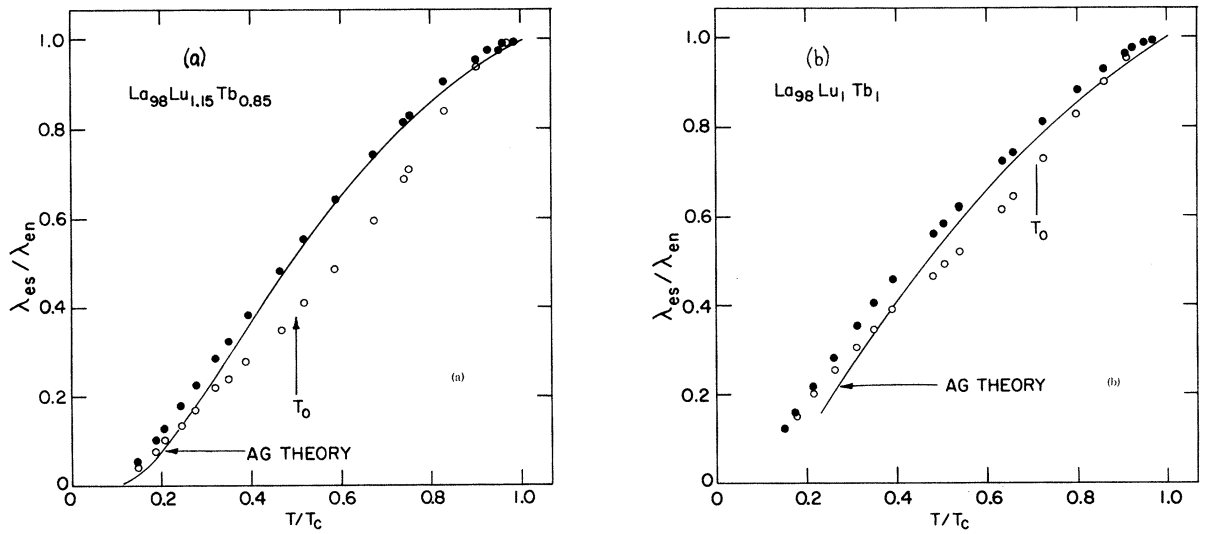

FIG. 5. Ratio of the electronic thermal conductivities for two different assumptions about the phonons. Solid circles assume $R_g = 1$ for all temperatures. Open circles assume the R_g given by BRT.

shoulder on the lower-bound curve arises from the phonon fit and not from magnetic-order effects.

At low temperatures, where the boundary and dislocation scattering of phonons is the dominant term, $\lambda_{es}/\lambda_{en}$ lies somewhat above the AG theory indicating that there are more low-lying excitation states than the theory predicts.

Critical-Field Curves

An ac susceptibility technique was used to measure the critical field for these samples. Both the applied field and the measuring field (less than 1 Oe) were parallel to the axis of the cylindrical sample. Transition widths (50 to 100 Oe) were very nearly independent of temperature and seemed to reflect inhomogeneity in the specimen. Measuring fields were always kept small so that the phase transition takes place at the nucleation field H_{c3}. If the thermodynamic critical-field curve H_c is calculated from these H_{c3} data using the measured normal electrical resistivity and type-II theory,[12] then H_0 for the $La_{98}Lu_2$ is found to be 710 Oe in good agreement with the value derived from specific-heat measurements (798 Oe) for pure d-hcp La.[13] In this calculation, the pure-metal value of κ, κ_0, was estimated to be 0.71 and κ values were calculated from $\kappa = \kappa_0 + 7.5\times10^3 \rho\sqrt{\gamma}$ (see Table I). The temperature dependence of κ was taken from Maki[11] and the ratio of H_{c3}/H_{c2} was taken to be 1.695.[14] This close agreement of the thermodynamic critical field to the specific-heat value lends support to our interpretation of the phase transition as the nucleation field H_{c3} rather than H_{c2}.

Critical-field curves shown on Fig. 6 are qualitatively very similar to the results of Crow, Guertin, and Parks[15] for the $InLa_{3-x}Gd_x$ system. $H_{c3}(0)$ appears to be depressed very rapidly for small impurity concentration and levels off at higher values. For samples 2 and 3, the critical-field curves are also very slightly reentrant. This reentrant character does not show up clearly on Fig. 6, but $H_{c3}(T)$ actually decreases about 1% as the temperature is lowered from 1.0 to 0.3 °K for samples 2 and 3. Theoretical predictions from the multiple-pair-breaking theory[16] are shown by the solid lines in Fig. 6. Near T_c the slope of the critical-field curve is close to the theory but at lower temperatures the measured value is only about half the theoretical prediction. Presumably, the difference between the measured critical-field curve and the simple multiple-pair-breaking theory arises from the exchange-field effects discussed by Bennemann, Garland, and Mueller.[17] These exchange fields can greatly enhance the effect of the applied field and are very detrimental to superconductivity.

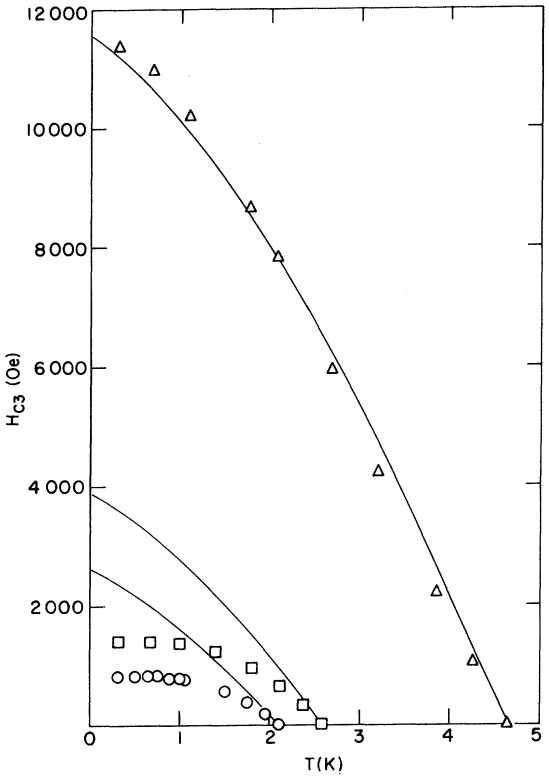

FIG. 6. Critical-field curves. Solid lines show the prediction of the multiple-pair-breaking theory.

REMARKS

For the materials which we have investigated, the major effects of magnetic impurities are adequately described by the simple lifetime broadening theory of Abrikosov-Gor'kov. The appearance of short-range order in the magnetic-impurity spin system does not seem to alter the superconducting properties by more than a few percent, as long as there is no applied field. Large deviations from the theory occur, however, in the presence of an external field because there is an enhancement from the exchange field. The enhancement factor is about a factor of 2 for these samples at low temperatures.

*Work was performed at the Ames Laboratory of the U. S. Atomic Energy Commission. Contribution No. 2707.

†Present address: Physics Department, University of Southern California, University Park, Los Angeles, Calif. 90007.

‡Present address: Physical Science Department, Western New Mexico University, Silver City, N. M 88061.

[1]K. H. Bennemann and F. M. Mueller, Phys. Rev. 176, 546 (1968).
[2]R. L. Cappelletti and D. K. Finnemore, Phys. Rev. 188, 723 (1969).
[3]A. A. Abrikosov and L. P. Gor'kov, Zh. Eksperim. i Teor. Fiz. 39, 178 (1960) [Soviet Phys. JETP 12, 1243 (1961)]; V. Ambegaokar and A. Griffin, Phys. Rev. 137, A1151 (1965).
[4]N. E. Phillips and B. T. Matthias, Phys. Rev. 121, 105 (1961); D. K. Finnemore, D. C. Hopkins, and P. E. Palmer, Phys. Rev. Letters 15, 891 (1965).
[5]D. K. Finnemore, L. J. Williams, F. H. Spedding, and D. C. Hopkins, Phys. Rev. 176, 712 (1968).
[6]W. R. Decker and D. K. Finnemore, Phys. Rev. 172, 430 (1968).
[7]P. Lindenfeld and W. B. Pennebaker, Phys. Rev. 127, 1881 (1962); A. B. Pippard, Phil. Mag. 46, 1104 (1955).
[8]J. Bardeen, G. Rickayzen, and L. Tewordt, Phys. Rev. 113, 982 (1959).
[9]P. G. Klemens, Proc. Roy. Soc. (London) A68, 1113 (1955).
[10]G. A. Slack, Phys. Rev. 105, 832 (1957).
[11]L. J. Williams, Ph. D. thesis (unpublished).
[12]K. Maki, Physics 1, 21 (1964).
[13]D. L. Johnson and D. K. Finnemore, Phys. Rev. 158, 376 (1966).
[14]D. Saint James and P. G. deGennes, Phys. Letters 7, 306 (1963).
[15]J. E. Crow, R. P. Guertin, and R. D. Parks, Phys. Rev. Letters 19, 77 (1967).
[16]P. Fulde and K. Maki, Phys. Rev. 141, 275 (1966).
[17]K. H. Bennemann, J. W. Garland, and F. M. Mueller, Phys. Rev. Letters 23, 169 (1969).

PHYSICAL REVIEW B VOLUME 2, NUMBER 5 1 SEPTEMBER 1970

Low-Field Magnetic Susceptibility of Gallium at Low Temperatures*

M. Hanabusa, A. H. Silver, † and Toshimoto Kushida
Scientific Research Staff, Ford Motor Company, Dearborn, Michigan 48121
(Received 29 April 1970)

The low-field static susceptibility of high-purity gallium was found to be strongly field and temperature dependent at low temperature. The change of the magnetic induction induced by a small field change was measured by using a superconducting quantum interference device. The observed susceptibility decreased markedly when the temperature was lowered from 4.2 to 1.5 °K; this corresponds to a susceptibility decrease of 7×10^{-4} cgs. A part of the decrease was recovered with an applied magnetic field less than $\frac{1}{2}$ Oe. The results of this static-susceptibility measurement seem to exclude any of the transport-phenomenon-type interpretations to explain the anomalous magnetoresistance previously observed for gallium. The present result strongly suggests an onset of extremely field-sensitive localized diamagnetic centers at low temperature.

I. INTRODUCTION

Transport properties of pure gallium exhibit anomalous behavior at low temperature. They are extremely sensitive to the magnetic field. Newbower and Neighbor reported a strongly field-sensitive magnetoresistance.[1] Previous to their work, Cochran and Shiffman[2] observed that the rf surface reactance of this metal changes sharply as a function of weak external field at low temperature. Boughton and Yaqub[3] found a similar anomaly in the thermal conductivity. Recently, one of the authors[4] conducted a detailed study on the field and the temperature dependence of the surface resistance of this metal with a marginal-oscillator detector. The work by Newbower and Neighbor is a dc measurement; so is the observation by Boughton and Yaqub. The studies in Refs. 2 and 4 are an rf surface impedance measurement. All of these observations are, however, closely related, and it is believed that one and the same mechanism is responsible for these anomalies. Since the rf measurement is a great deal simpler and more sensitive, most extensive information has been obtained using this method.[4]

Although the details of the rf resistivity measurements will be published in a forthcoming paper, the essential properties of the anomaly are summarized as follows:

(i) This is an essentially frequency-independent phenomenon (from dc to at least 100 MHz).

(ii) The effect is independent of sample size.

(iii) The anomaly is not associated with a bulk phase transformation, as was evidenced by a nuclear-quadrupole-resonance study.[5] This was also supported by a specific-heat measurement.[6]

(iv) A very small amount of gas contamination is responsible for this anomaly. A carefully outgassed sample shows no or very weak anomaly.[4]

(v) There is a definite onset temperature T_c for the anomaly. Below T_c the magnitude of the anomaly increases as the temperature decreases. The